Euro. Jnl of Applied Mathematics (2014), *vol.* 25, *pp.* 729–747. © Cambridge University Press 2014
doi:10.1017/S0956792514000242

Conformal mapping, Padé approximants, and an example of flow with a significant deformation of the free boundary

E. A. KARABUT and A. A. KUZHUGET

Lavrentyev Institute of Hydrodynamics, Siberian Branch, Russian Academy of Sciences,
Novosibirsk State University
630090 Novosibirsk, Russia
email: eakarabut@gmail.com

(*Received 6 August 2013; revised 8 July 2014; accepted 11 July 2014; first published online 7 August 2014*)

A problem of plane inertial motion of an ideal incompressible fluid with a free boundary, which initially has a quadratic velocity field, is studied by semi-analytical methods. A conformal mapping of the domain occupied by the fluid onto a unit circle is sought in the form of a power series with respect to time. Summation of series is performed by using Padé approximants.

Key words: Conformal mapping; Padé approximant; Free boundary flow; Ideal incompressible fluid

1 Introduction

A plane unsteady potential flow of an ideal incompressible fluid with a free boundary is considered. In the case considered, there are no external forces and no surface tension.

At each time t, the fluid occupies a certain bounded simply connected domain in the plane of the complex variable $Z = x + \mathrm{i}y$. The domain boundary is free, and a zero pressure is maintained on this boundary. The domain at the initial time $t = 0$ is known. The subsequent motion of the fluid has a purely inertial nature and is induced by a given initial velocity field. The goal is to find the domain shape and the velocity field at $t > 0$.

Such a problem with a free boundary does not have many examples of exact solutions. The only known class of non-one-dimensional exact solutions contains flows with a linear velocity field (the velocity components u and v are linear functions of x and y). This class of flows was discovered by Dirichlet in 1857 [6]. The fluid was assumed to be self-gravitating; a particular case without gravity was later studied in [15–17, 20, 22, 27]. For plane potential flows with a linear velocity field, the free surface in the absence of gravity is a second-order curve: hyperbola, ellipse, parabola, or straight line in the degenerate case.

A small number of exact solutions may suggest that not all exact solutions have been found. This is confirmed by a large number of exact solutions in similar flows with a free boundary for viscous fluids: Hele-Shaw flows and plane Stokes flows. The first examples of such exact solutions were obtained in 1945 [8, 26]. Some of the numerous subsequent examples were presented in [4].

An attempt to find new exact solutions in a plane problem of motion of an ideal fluid with a free boundary and a nonlinear velocity field was made in [14] and in this work. The main idea of these two investigations was to use simple initial conditions. In both works, the initial complex velocity $U = u - iv$ is identical: it is a quadratic function of Z, but the initial domains occupied by the fluid are different: a wedge in [14] and a unit circle in this work. The exact solution was found in [14], but the exact solution of the problem considered below is still unavailable. Its semi-analytical solution is demonstrated in this paper.

A quadratic initial velocity field is indeed the simplest case. If a linear initial velocity is taken for a wedge or a circle, the solution is trivial: the wedge transforms with time to another wedge (the wedge apex angle is a function of time), and the circle transforms into an ellipse. In both cases, the velocity field remains linear for all time.

An exact solution of the problem of deformation of a fluid wedge with an apex angle α, which has a quadratic initial velocity field, was found in [14] by using a technique successfully used previously in the problem of gravity waves on a fluid surface [12, 13]. This technique is based on an analytical continuation of the unknown function beyond the boundary of the domain of definition of the function. After multiple passing around the wedge apex, different branches of the sought function become related, generally speaking, by an infinite system of ordinary differential equations. It was demonstrated that the system becomes finite if α/π is a rational number. For some angles α, the solution of this system could be found in an explicit form. A new class of self-similar flows with a free boundary whose velocity field differs from a linear field was found.

This present work is based on three ideas previously put forward by various researchers:

- application of conformal mapping for describing plane flows;
- presentation of the solution in the form of power series in time;
- application of semi-analytical methods.

Let there be a certain canonical domain in an auxiliary plane ζ. We search for a conformal mapping of this domain onto the domain occupied by the fluid. This approach offers some advantages over traditional methods. Instead of the boundary-value problem in an unknown domain with a moving boundary, we obtain a boundary-value problem with a fixed boundary in the plane ζ.

The boundary conditions for two sought functions, i.e., the conformal mapping $Z(\zeta, t)$ and complex potential $\Phi(\zeta, t)$, were obtained in [24]. It turned out that they are cubically nonlinear conditions, which is not very convenient for seeking the solution in the form of power series with respect to time: recurrent formulas for sequentially finding the terms of the series contain double sums.

It was noted [10] that the boundary conditions become quadratically nonlinear if another pair of function is used: the conformal mapping $Z(\zeta, t)$ and complex velocity $U(\zeta, t) = \Phi_\zeta / Z_\zeta$. This is more convenient because the recurrent formulas become simpler: they contain only single sums.

Using one more pair of functions $R(\zeta, t) = 1/Z_\zeta$ and $U(\zeta, t)$ was proposed in [7]. In this case, using the boundary conditions, one can derive cubically nonlinear operator

https://doi.org/10.1017/S0956792514000242 Published online by Cambridge University Press

equations resolved with respect to the derivatives R_t and U_t. Therefore, there is no need to use division operations in calculating R_t and U_t. The algorithm for solving the problem is substantially simplified. This approach is widely used for studying long-time evolution of water waves [7, 33].

The problem of a spherical bubble ascending in a liquid was studied in [23] with the use of power series in time. The convergence of the series in this problem was proved in [3]. The possibility of using power series in time for conformal mapping is based on the theorems of existence and uniqueness proved in [24]. Various plane problems of ascending or inertial motion of a cylindrical bubble with the use of power series in time were considered in [2, 9, 11, 21]. Both conformal mapping and semi-analytical methods were used in this articles. Cumulative jets were observed to form in all problems of bubble motion. Cumulation is a phenomenon of energy concentration either in a certain place or in a certain direction. In the problem considered below, there are three cumulative jets, which induce significant deformation of the free boundary. Other examples of cumulative jet formation in a liquid obtained by finite-difference methods can be found in [25].

Semi-analytical methods (the name was proposed by M. Van Dyke [30–32]) are mainly methods of computer processing of power series. They occupy an intermediate position between numerical and analytical methods. In addition to high accuracy of calculations, semi-analytical methods sometimes provide unique analytical information, which can be difficult to obtain by purely numerical and by purely analytical methods; sometimes obtaining this information is impossible altogether. Semi-analytical methods are mainly used to solve two problems: analytical continuation of the power series beyond the circle of its convergence and finding the locations and types of singularities. Padé approximants, continued fractions, Padé diagrams, Domb-Sykes test, algorithms for convergence acceleration, and other methods are used to solve these problems.

There are numerous examples of effective applications of semi-analytical methods in problems with a free boundary. For instance, in the problem of water waves, the first publication was [18], and one of the most recent examples is [5]. In [18], semi-analytical methods were used to discover nonmonotonicity of wave parameters due to amplitude variations. In [5], fine nonlinear effects for waves with an almost-highest amplitude were studied. These effects were previously detected earlier, in [19], by finite-difference methods.

The conformal mapping and complex velocity are sought below in the form of power series in time. The convergence of the power series and the accuracy of the calculation are carefully analyzed. A new algorithm is used to find the radius of convergence. This is based on finding the zeroes of the partial sums of the series. With the use of the Padé approximants, the power series are summed up to times that are ten-fold greater than the radius of convergence. The free surface and the velocity of the fluid are found.

Conformal mappings have the following inherent defect. If the domain experiences significant deformations, then the function performing the conformal mapping becomes a rapidly changing function and can be hard to use in numerical modelling. In this work, we demonstrate a method for correcting this defect in the case where the solution is sought in the form of a power series in time. The method is based on a certain change of variables, also in the form of a power series.

2 Conformal mapping

Let us consider a unit circle $|\zeta| < 1$ in an auxiliary plane ζ. We search for a function $Z(\zeta, t)$, which is a conformal mapping of the circle $|\zeta| < 1$ onto the domain occupied by the fluid (see Figure 1), and for the complex velocity $U(\zeta, t)$. There are two boundary conditions on the free boundary $|\zeta| = 1$.

The first (kinematic) boundary condition means that the projection of the velocity $\overline{U}$ of the fluid particle located on the free boundary onto the normal to the free boundary coincides with the projection of the velocity of the boundary itself Z_t to the same normal. In other words, the vector $Z_t - \overline{U}$ is directed tangentially to the free surface. As $\zeta = \mathrm{e}^{\mathrm{i}\theta}$ on the free surface, the normal vector is $\mathrm{i}Z_\theta$, and the scalar product of the vectors Z_1 and Z_2 is given by the formula $\mathrm{Re}\, Z_1\overline{Z_2}$, then we obtain the kinematic condition in the following form:

$$\mathrm{Im}\,[Z_\theta(\overline{Z_t} - U)] = 0. \tag{2.1}$$

The second (dynamic) boundary condition can be obtained from the condition of orthogonality of acceleration to the free surface. For convenience, we denote the times in the Eulerian and Lagrangian coordinates by τ and T, respectively. Then the dynamic condition can be written in the following form:

$$\mathrm{Re}\, Z_\theta U_T = 0. \tag{2.2}$$

Let us find the acceleration U_T. As Z and τ are independent variables, we obtain

$$Z_\tau = Z_t + Z_\zeta \zeta_\tau = 0.$$

Therefore, we have

$$\frac{\partial}{\partial \tau} = \frac{\partial}{\partial t} + \zeta_\tau \frac{\partial}{\partial \zeta} = \frac{\partial}{\partial t} - \frac{Z_t}{Z_\zeta}\frac{\partial}{\partial \zeta}.$$

In addition, taking into account that

$$\frac{\partial}{\partial T} = \frac{\partial}{\partial \tau} + Z_T \frac{\partial}{\partial Z} = \frac{\partial}{\partial \tau} + \overline{U}\frac{\partial}{\partial Z}, \quad \frac{\partial}{\partial Z} = \frac{1}{Z_\zeta}\frac{\partial}{\partial \zeta},$$

we obtain the following formula for acceleration:

$$U_T = U_t - \frac{Z_t}{Z_\zeta}U_\zeta + \frac{\overline{U}}{Z_\zeta}U_\zeta.$$

Substituting it into (2.2) and then replacing the operator $\partial/\partial\theta$ by $\mathrm{i}\zeta\partial/\partial\zeta$ in (2.1) and (2.2), we obtain

$$\mathrm{Im}\,\zeta(Z_\zeta U_t - U_\zeta Z_t + U_\zeta \overline{U}) = 0, \quad \mathrm{Re}\,(\zeta Z_\zeta U - Z_t\overline{Z_\zeta}/\zeta) = 0, \quad |\zeta| = 1\,. \tag{2.3}$$

Thus, there are two boundary conditions (2.3) for finding two analytical functions $Z(\zeta, t)$ and $U(\zeta, t)$.

The solution is sought in the form of a power series in time:

$$Z(\zeta, t) = Z^{(0)}(\zeta) + Z^{(1)}(\zeta)t + Z^{(2)}(\zeta)t^2 + \cdots, \tag{2.4}$$

https://doi.org/10.1017/S0956792514000242 Published online by Cambridge University Press

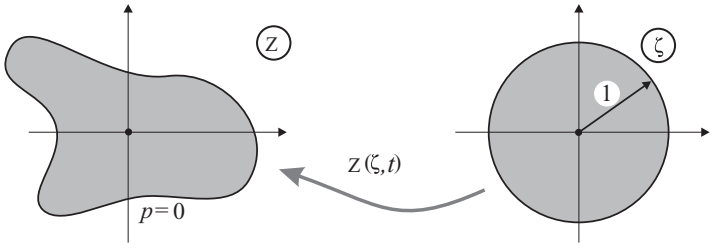

FIGURE 1. Conformal mapping of a unit circle in the plane ζ onto the flow domain in the physical plane Z. A zero pressure p is maintained on the free surface.

$$U(\zeta,t) = U^{(0)}(\zeta) + U^{(1)}(\zeta)t + U^{(2)}(\zeta)t^2 + \cdots. \tag{2.5}$$

The series coefficients with index zero, which define the initial shape of the domain and the initial velocity field, take the form

$$Z^{(0)}(\zeta) = \zeta, \quad U^{(0)}(\zeta) = \zeta^2.$$

Thus, the initial domain occupied by the fluid is a unit circle, and we have a quadratic initial velocity field. The streamlines and the velocity vector at $t = 0$ are shown in Figure 2. The absolute value of the velocity vector on the free surface is independent of position and equal to unity; it is only the velocity direction that changes.

The subsequent coefficients $Z^{(n+1)}$ and $U^{(n+1)}$ are found from the recurrent boundary conditions

$$(n+1)\mathrm{Im}\,\zeta U^{(n+1)} Z_\zeta^{(0)} = \mathrm{Im}\,\zeta \left(\sum_{j=0}^{n} (j+1) U_\zeta^{(n-j)} Z^{(j+1)} - \sum_{j=0}^{n-1} (j+1) Z_\zeta^{(n-j)} U^{(j+1)} - \sum_{j=0}^{n} \overline{U^{(n-j)}} U_\zeta^{(j)} \right), \tag{2.6}$$

$$(n+1)\mathrm{Re}\,Z^{(n+1)} \overline{Z_\zeta^{(0)}}/\zeta = \mathrm{Re}\,\zeta \left(\sum_{j=0}^{n} Z_\zeta^{(n-j)} U^{(j)} - \sum_{j=1}^{n} (n-j+1) \overline{Z^{(n-j+1)}} Z_\zeta^{(j)} \right). \tag{2.7}$$

Boundary conditions (2.6) and (2.7) are obtained by substituting series (2.4), (2.5) into (2.3).

Using consecutively (2.6) and (2.7), we obtain

$$Z(\zeta,t) = \zeta + \zeta^4 t + (-2\zeta + 3\zeta^7)t^2 + (-12\zeta^4 + 12\zeta^{10})t^3 + \cdots, \tag{2.8}$$

$$U(\zeta,t) = \zeta^2 + 2\zeta^5 t + (-7\zeta^2 + 7\zeta^8)t^2 + (-36\zeta^5 + 30\zeta^{11})t^3 + \cdots. \tag{2.9}$$

If we eliminate ζ in series (2.8), (2.8) we can obtain a representation of $U(Z,t)$ in the form of a power series with respect to t:

$$U(Z,t) = Z^2 - 3Z^2t^2 - 2Z^5t^3 + 18Z^2t^4 + \frac{108}{5}Z^5t^5 - \left(\frac{536}{5}Z^2 - 6Z^8\right)t^6 + \cdots.$$

https://doi.org/10.1017/S0956792514000242 Published online by Cambridge University Press

Table 1. *Coefficients of the power series for conformal mapping*

$Z(\zeta,t)$	ζ^1	ζ^4	ζ^7	ζ^{10}	ζ^{13}	ζ^{16}	ζ^{19}	ζ^{22}	ζ^{25}
t^0	1								
t^1	0	1							
t^2	−2	0	3						
t^3	0	−12	0	12					
t^4	$\frac{29}{2}$	0	−71	0	55				
t^5	0	$\frac{782}{5}$	0	−430	0	273			
t^6	$-\frac{568}{5}$	0	$\frac{2681}{2}$	0	−2652	0	1428		
t^7	0	$-\frac{65\ 826}{35}$	0	$\frac{374\ 708}{35}$	0	−16 576	0	7752	
t^8	$\frac{235\ 577}{280}$	0	$-\frac{1\ 520\ 431}{70}$	0	$\frac{5\ 758\ 467}{70}$	0	−104 652	0	43 263

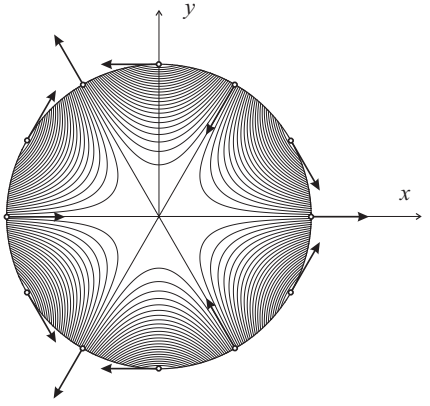

FIGURE 2. Streamlines of the flow and direction of the velocity vector at the initial time.

It turns out that the velocity field remains quadratic with accuracy to $O(t^3)$ at small values of t.

The subsequent coefficients of the power series (2.8), (2.9) are presented in Tables 1 and 2. A total of 600 terms of these power series were found in rational numbers (the computation on a laptop lasted for two days).

Beginning from the 601st term, the computations by recurrent formulas were performed in real numbers with the initial mantissa length of 1000 decimal digits. In long-time computations, the accuracy gradually decreases because of rounding errors. We managed to find 1100 terms of the series, and the last terms had the accuracy already of 100 decimal digits (one day of computations). The idea to obtain as many coefficients as possible has a simple explanation: the greater the number of coefficients found, the greater the time for which the solution can be constructed.

3 Direct summation of power series

Let us consider the power series (2.4) on the free surface, i.e., at $\zeta = e^{i\theta}$. For a given value of the parameter θ, we find 150 terms of series (2.4). Summing them up at a certain value

https://doi.org/10.1017/S0956792514000242 Published online by Cambridge University Press

Table 2. *Coefficients of the power series for the complex velocity*

$U(\zeta,t)$	ζ^2	ζ^5	ζ^8	ζ^{11}	ζ^{14}	ζ^{17}	ζ^{20}	ζ^{23}	ζ^{26}
t^0	1								
t^1	0	2							
t^2	−7	0	7						
t^3	0	−36	0	30					
t^4	63	0	−209	0	143				
t^5	0	$\frac{2757}{5}$	0	−1262	0	728			
t^6	$-\frac{2817}{5}$	0	$\frac{22\ 414}{5}$	0	−7787	0	3876		
t^7	0	$-\frac{261\ 224}{35}$	0	$\frac{243\ 931}{7}$	0	−48 736	0	21 318	
t^8	$\frac{335\ 669}{70}$	0	$-\frac{2\ 803\ 172}{35}$	0	$\frac{9\ 217\ 184}{35}$	0	−308 142	0	120 175

of t, we obtain a point in the plane Z. As θ changes from 0 to 2π, this point describes a closed curve in the plane Z. These curves are shown in Figure 3.

The free surface remains smooth as long as the numerical power series for each point of the free surface remain convergent. As soon as this condition is violated at a certain point of the free boundary, the partial sum of the series becomes a large number. Then there is a significant deformation of the free surface in the vicinity of this point, which has no physical meaning. The emergence of such rapidly growing distortions of the free boundary testifies to divergence of the series.

It is seen that the series converges at $t = 0.06$. The free surface is smooth everywhere, and the initial circumference is slightly deformed. The greatest time at which the series converges at all points of the free surface is $t = 0.123$. The deformation is greater now, although it still remains rather small. At $t = 0.125$, the series diverges at those points of the free boundary where the values of the parameter θ is close to $\pi/6 + \pi k/3$, $k \in \mathbb{Z}$. Distortions on the free surface appear and then increase at $t = 0.126$. With a further increase in time, the distortions rapidly grow and completely cover the free boundary areas where the power series converges. To see these areas, we sum up the series only at 180 points of the free boundary ($\theta = j\pi/90$; $j = 0, 1, \ldots, 180$). Each summation yields a complex number, which is shown as a small circle in Figure 3. At $t = 0.15$, the free surface "falls apart": it ceases to be smooth, and most of the points go outside the figure. This means that the series diverges. The greatest radius of convergence of the series is observed at six points with the minimum and maximum curvature of the free surface. There are small isles of stability here: the circles are grouped into smooth lines. At $t = 0.19$, an even greater number of circles are outside the figure, but it is still possible to guess the overall contour of the free surface.

For an arbitrary power series

$$f(t) = a_0 + a_1 t + a_2 t^2 + a_3 t^3 + \ldots \quad (t \in \mathbb{C}) \tag{3.1}$$

the radius of convergence is equal to the distance from the origin of the coordinate system $t = 0$ to the nearest singular point. The location of such a singular point is estimated by using either the Padé diagram or the well known theorem: if there is a limit $\lim_{n\to\infty} a_{n-1}/a_n = t_0$, then t_0 is a singular point of series (3.1).

https://doi.org/10.1017/S0956792514000242 Published online by Cambridge University Press

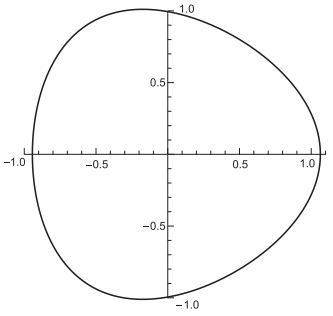

t=0.06

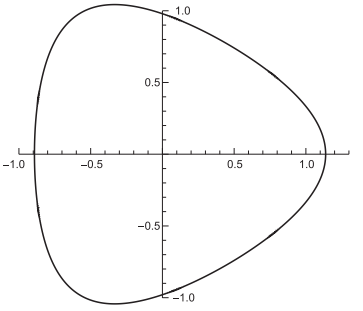

t=0.123

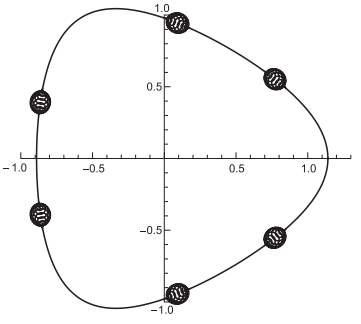

t=0.125

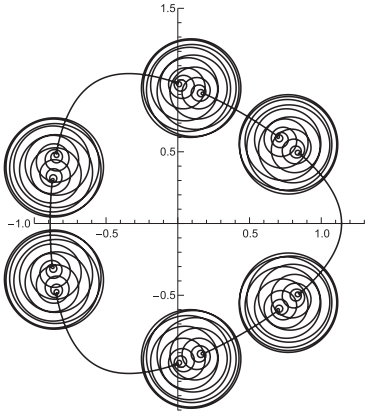

t=0.126

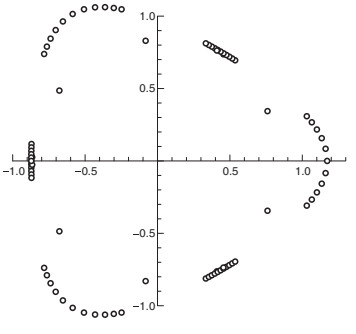

t=0.15

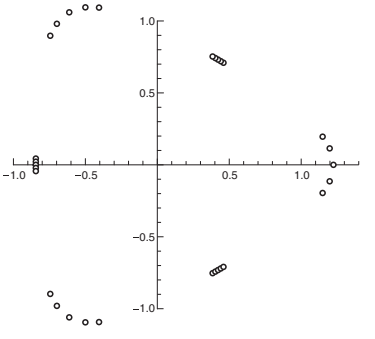

t=0.19

FIGURE 3. Free surface obtained by summation of the power series at different times.

https://doi.org/10.1017/S0956792514000242 Published online by Cambridge University Press

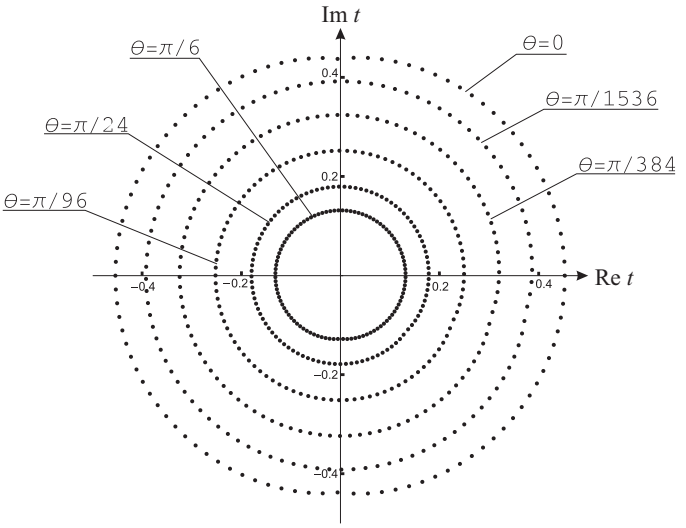

FIGURE 4. Zeros of partial sums of the series.

In this work, we propose a new graphical method based on the Jentzsch theorem [29]. According to this theorem, for all power series, each point of the boundary of the circle of convergence is a limiting point for zeroes of the partial sums of this series.

Figure 4 shows the roots of the equations

$$Z^{(0)}(e^{i\theta}) + Z^{(1)}(e^{i\theta})t + Z^{(2)}(e^{i\theta})t^2 + \cdots + Z^{(100)}(e^{i\theta})t^{100} = 0$$

for various values of θ in the plane of the complex time t. The roots are lined up uniformly along circumferences (approximately, but with good accuracy). This is a clear and precise method of visual presentation of the circles of convergence.

The radius of convergence of series (2.4) on the free surface is an even function of θ, which is periodic with a period $\pi/3$. Figure 4 shows the behaviour of the radius of convergence over a half period at $\theta \in [0, \pi/6]$. The greatest radius of convergence is reached at $\theta = 0$. After that, with a small increase in θ, the radius of convergence drastically decreases and reaches a minimum at $\theta = \pi/6$.

4 Padé approximants

The most famous and most popular method of analytical continuation of the power series beyond the circle of convergence is based on the use of the Padé approximants. Are two functions that have identical first terms of the Taylor series close to each other? The answer here is yes. If we take an arbitrary function and a polynomial that is a partial sum of its Taylor series, these two functions are close to each other in the circle of convergence of the Taylor series. If we take a more complicated function, e.g., a ratio of polynomials, instead of the polynomial, then the domain of closeness is not necessarily a circle; it can be greater than the circle of convergence.

https://doi.org/10.1017/S0956792514000242 Published online by Cambridge University Press

The Padé approximant is the ratio of polynomials of power L and M such that the first $L+M+1$ terms of the Taylor series are identical for the Padé approximant and the sought function. For an arbitrary function $f(t)$, we have the following definition of the Padé approximant:

$$f(t) = \sum_{n=0}^{\infty} a_n t^n = [L/M] + O(t^{L+M+1}),$$

where the symbol $[L/M]$ is used to denote the Padé approximant:

$$[L/M] = \frac{P_L(t)}{Q_M(t)}.$$

The numbers L and M can be arbitrary, and all Padé approximants are grouped into the Padé table:

$$\begin{array}{llll} [0/0] & [0/1] & [0/2] & \ldots \\ [1/0] & [1/1] & [1/2] & \ldots \\ [2/0] & [2/1] & [2/2] & \ldots \\ \multicolumn{4}{c}{\ldots\ldots\ldots\ldots\ldots\ldots\ldots\ldots\ldots\ldots\ldots\ldots} \end{array}$$

The greater the values of L and M, the higher the accuracy with which the Padé approximant describes the function $f(t)$. The case with $L = M$ is considered most frequently.

The Padé summation for power series is usually understood as considering the diagonal of the Padé table:

$$[0/0], \qquad [1/1], \qquad [2/2], \qquad [3/3], \qquad \ldots .$$

Such a diagonal sequence often tends to the function even outside the circle of convergence; therefore, the function can be estimated by taking the Padé approximant of a sufficiently high order.

Theorems of convergence of the Padé approximants were obtained for various classes of functions. For instance, the Stahl's theorem considers the case where the function has a finite number of branching points [28]. In this case, the function is multi-valued. However, the function can be made single-valued by drawing cuts from singular points. The Stahl theorem states that, if these cuts are drawn in a special manner (all cuts consist of a finite number of piecewise-analytical arcs), then the diagonal sequence of the Padé approximants converges to a function in the exterior of these cuts. For instance, for the function $f(z) = 1/\sqrt{z^2-1}$, the convergence occurs in the exterior of the segment connecting the points $z = \pm 1$. The exact formulations of the Stahl theorem and other theorems can be found in the review [1].

Let us first study the convergence of the Padé approximants for series (2.4) at the free surface point $\zeta = 1$:

$$Z(1,t) = 1 + t + t^2 - \frac{3}{2}t^4 - \frac{3}{5}t^5 + \frac{29}{10}t^6 + \frac{6}{5}t^7 - \cdots.$$

https://doi.org/10.1017/S0956792514000242 Published online by Cambridge University Press

Table 3. *Diagonal sequence of the Padé approximants for the function* $Z(1,t)$ *at* $t = 1$

[40/40]	**2.46106** 00251846022457
[50/50]	**2.46106** 48872561470996
[60/60]	**2.4610650** 806608559623
[70/70]	**2.46106507** 88733588925
[80/80]	**2.46106507913** 15438477
[90/90]	**2.461065079137** 8731968
[100/100]	**2.461065079137** 8819368
[110/110]	**2.46106507913793** 57731
[120/120]	**2.46106507913793** 62611
[130/130]	**2.46106507913793** 29822
[140/140]	**2.461065079137933021** 8
[150/150]	**2.461065079137933021** 6
[160/160]	**2.461065079137933021**

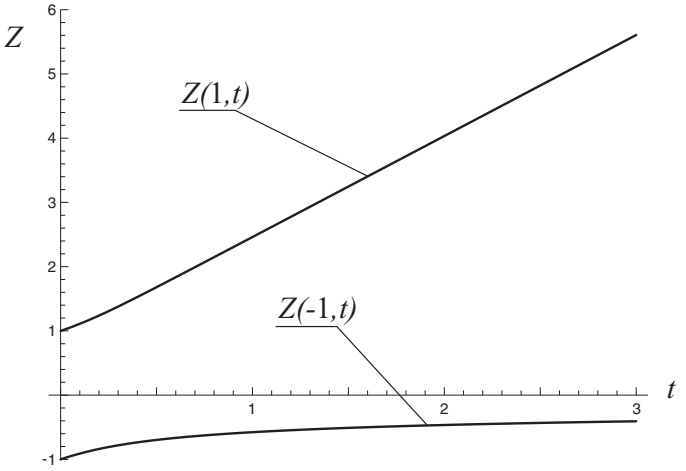

FIGURE 5. Motion of two opposite points on the free surface.

We transform this numerical series to the Padé approximant. Table 3 shows the diagonal sequence $\{[L/L]\}$ taken at $t = 1$. The correctly computed digits are printed in bold. Good convergence of the sequence is observed as $L \to \infty$. At $t > 1$, convergence also occurs, but at a slower rate. Similarly, it is possible to check that convergence also occurs at $\zeta = -1$.

Figure 5 shows the coordinates of the point $\zeta = 1$ and the opposite point $\zeta = -1$ as functions of time. At $\zeta = 1$, the curve has an inclined asymptote. Thus, at very large times, the point $\zeta = 1$ moves with a constant velocity. The dependence of velocity on time is shown in Figure 6. The following limits are found: $\lim_{t\to\infty} U(1,t) = 1.5734$ and $\lim_{t\to\infty} U(-1,t) = 0$. The approximants [300/300] were used to construct Figures 5 and 6.

Is a cusp formed on the free surface? The time evolution of the maximum curvature of the free surface k reached at the point $\zeta = 1$ is shown in Figure 7 in a logarithmic scale. The curve is smooth everywhere, and a cusp is not formed at least until the time $t = 11$. The approximant [500/500] was used to construct Figure 7.

https://doi.org/10.1017/S0956792514000242 Published online by Cambridge University Press

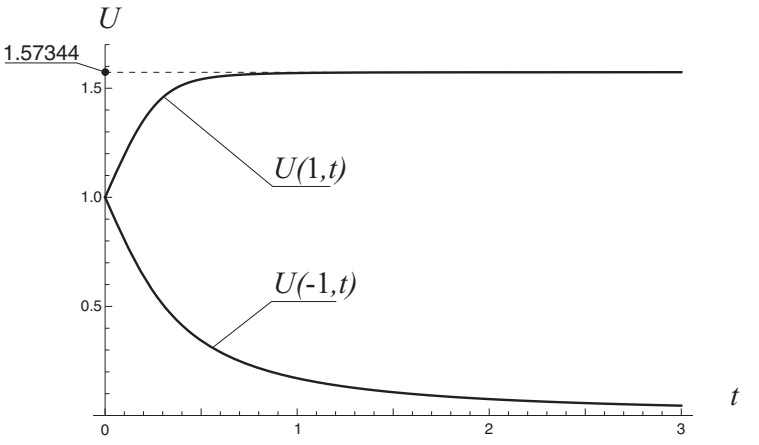

FIGURE 6. Velocity at two points of the free surface versus time.

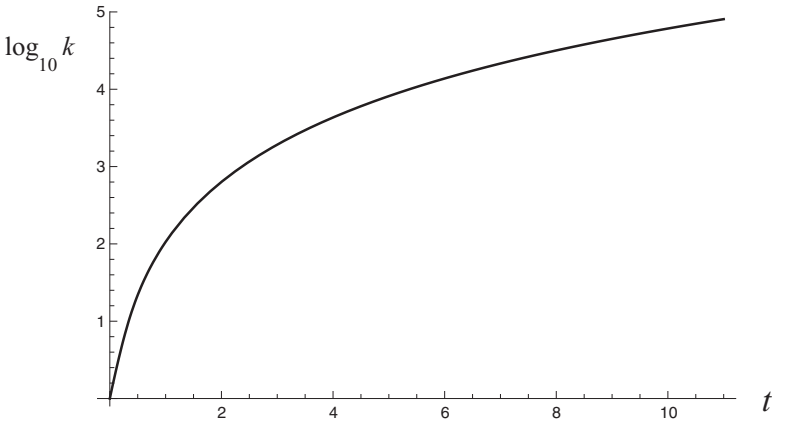

FIGURE 7. Curvature of the free surface k at the point $\zeta = 1$ versus time.

Figure 8 demonstrates the convergence of the Padé approximants at points of the free boundary other than $\zeta = \pm 1$. Here we specially choose two time instants that were already used to construct the free surface by means of direct summation of the series in Figure 3. We again take 180 points ($\theta = j\pi/90;\ j = 0, 1, \ldots, 180$) and construct a power series (2.4) for each point. After that, for each series, we find the approximant [150/150] and calculate it at $t = 0.19$. The resultant points are shown in Figure 8. In Figure 3, most of the markers are outside the figure at $t = 0.19$. In Figure 8, all 180 markers "returned" to their places: they are located along the free boundary. At $t = 0.126$, Figure 8 shows the curve given by the Padé approximant [150/150] for a continuous change in θ from 0 to 2π. A comparison with Figure 3 shows that the Padé summation, in contrast to the usual summation, "removes" regions of instability of the free boundary without changing the smooth areas of the boundary.

https://doi.org/10.1017/S0956792514000242 Published online by Cambridge University Press

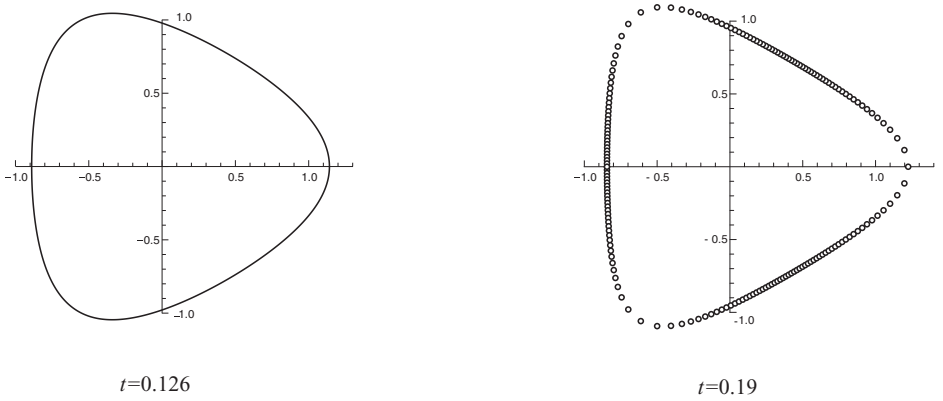

t=0.126 t=0.19

FIGURE 8. Free surface obtained by the Padé summation of the power series.

5 Replacement of variables

With increasing t, the rate of convergence of the Padé approximants decreases, but in principle the Padé summation allows one to construct the free surface for all time. However, finding the free boundary with acceptable accuracy may require an extremely large number of terms of the initial power series.

A more series obstacle in constructing the free boundary is the problem noticeable already at $t = 0.19$ in Figure 8. The points ζ are located uniformly on the unit circumference $|\zeta| = 1$, but the images of these points in the plane Z are arranged nonuniformly. Moreover, there are few markers on those parts of the free boundary where the greatest deformations are observed and where we would like to have more markers. This tendency becomes even worse with increasing time. It is seen in Figure 9(a), which shows the free surface constructed by the Padé summation at $t = 1.5$. Almost all 180 markers are grouped along the smoothest part of the free boundary. There is only one marker in the vicinity of the point $\zeta = 1$ (point A in the figure). A large empty segment of the free boundary, which is not filled by markers, is formed. How is it possible to construct the free surface here?

One possible way is to arrange the points nonuniformly in the plane ζ. However, there are two problems here. The first problem is the fact that it is necessary to know the absolute value of the conformal mapping derivative $|Z_\zeta|$ to find out at which point of the plane ζ the marker should be placed. This value is also given by a power series in time, but this series is poorly converging. This is not surprising because of the value of $|Z_\zeta|$ becomes very large at large deformations of the free boundary. For instance, we have $|Z_\zeta| \sim 10^{22}$ at the point $\zeta = 1$ at $t = 1.5$. The second problem is the high sensitivity of the free surface to microscopic changes in the angle θ. For instance, the entire empty segment in Figure 9(a) in the vicinity of the point A corresponds to the change in the angle θ from -10^{-22} to 10^{-22}. In practice, it is possible to construct the free surface by means of direct Padé summation of series (2.4) only up to $t = 0.5$. At $t > 0.5$, this summation already requires significant computational effort.

https://doi.org/10.1017/S0956792514000242 Published online by Cambridge University Press

Table 4. *Coefficients of the power series for the free surface after change of variables*

$Z(\mu,t)$	μ^{-14}	μ^{-11}	μ^{-8}	μ^{-5}	μ^{-2}	μ	μ^4	μ^7	μ^{10}	μ^{13}	μ^{16}
t^0						1					
t^1					$\frac{2}{3}$	0	$\frac{1}{3}$				
t^2				$\frac{11}{36}$	0	$\frac{2}{9}$	0	$\frac{17}{36}$			
t^3			$\frac{31}{81}$	0	$\frac{5}{27}$	0	$-\frac{41}{27}$	0	$\frac{77}{81}$		
t^4		$\frac{2633}{3888}$	0	$-\frac{1469}{972}$	0	$\frac{2203}{1296}$	0	$-\frac{4487}{972}$	0	$\frac{4375}{1944}$	
t^5	$\frac{41\ 723}{29\ 160}$	0	$-\frac{21\ 485}{5832}$	0	$\frac{1979}{7290}$	0	$\frac{35\ 126}{3645}$	0	$-\frac{82\ 267}{5832}$	0	$\frac{170\ 617}{29\ 160}$

In this paper, we propose a new method of constructing the free boundary. Instead of series (2.4), we propose to use another series:

$$Z(\mu,t)=\mu+t\left(\frac{2}{3\mu^2}+\frac{\mu^4}{3}\right)+t^2\left(\frac{11}{36\mu^5}+\frac{2\mu}{9}+\frac{17\mu^7}{36}\right)+\cdots. \tag{5.1}$$

The subsequent coefficients of this series are listed in Table 4. A total of 200 terms of series (5.1) in rational numbers were found (two days of computations on a laptop).

In the plane of the complex variable μ, we take 180 points $\mu=\mathrm{e}^{\mathrm{i}\alpha}$ ($\alpha=j\pi/90$; $j=0,1,\ldots,180$) uniformly arranged on the unit circumference $|\mu|=1$ and form a power series (5.1) for each point. After that, for each series, we find the approximant [100/100] and calculate it at $t=1.5$. The thus-found points are shown in Figure 9(b). It is seen that the resultant free surface coincides with the free surface in Figure 9(a). In contrast to Figure 9(a), however, there are no empty places in the vicinity of the points A, B, and C. Series (5.1) has a remarkable property: the images of the points uniformly arranged on the circumference $|\mu|=1$ are uniformly arranged on the free surface as well.

We have two functions $Z(\zeta,t)$ and $Z(\mu,t)$. The first function is an analytical function of the complex variable ζ, and the second function is an analytical function of the complex variable μ. However, the first function is a holomorphic function in the circle $|\zeta|\leqslant 1$, whereas the second function, generally speaking, is not a holomorphic function in the circle $|\mu|\leqslant 1$. We show how it is possible to find a complex replacement $\mu(\zeta,t)$ so that the function $Z(\zeta,t)$ given by series (2.4) could be obtained by substituting this replacement into the function $Z(\mu,t)$ given by series (5.1).

The idea of obtaining series (5.1) is simple. The function $Z(\theta,t)$, where $\theta\in[0,2\pi]$, which given a parametric presentation of the free boundary, is not a unique function. If we replace the variables as $\theta=\theta(\alpha,t)$, where θ is a monotonic function of α and the parameter α changes from 0 to 2π, we obtain a new function $Z(\alpha,t)$, which describes the same free boundary. We only have to find the replacement of the variables at which the points uniformly arranged on the segment $\alpha\in[0,2\pi]$ are uniformly arranged on the free boundary as well.

The parameter α is taken as a linear function of S:

$$\alpha=2\pi S/S_0. \tag{5.2}$$

Here S is the length of the free boundary counted from the point $\zeta=1$ and S_0 is the total length of the free boundary. Obviously, such a choice ensures uniform arrangement

https://doi.org/10.1017/S0956792514000242 Published online by Cambridge University Press

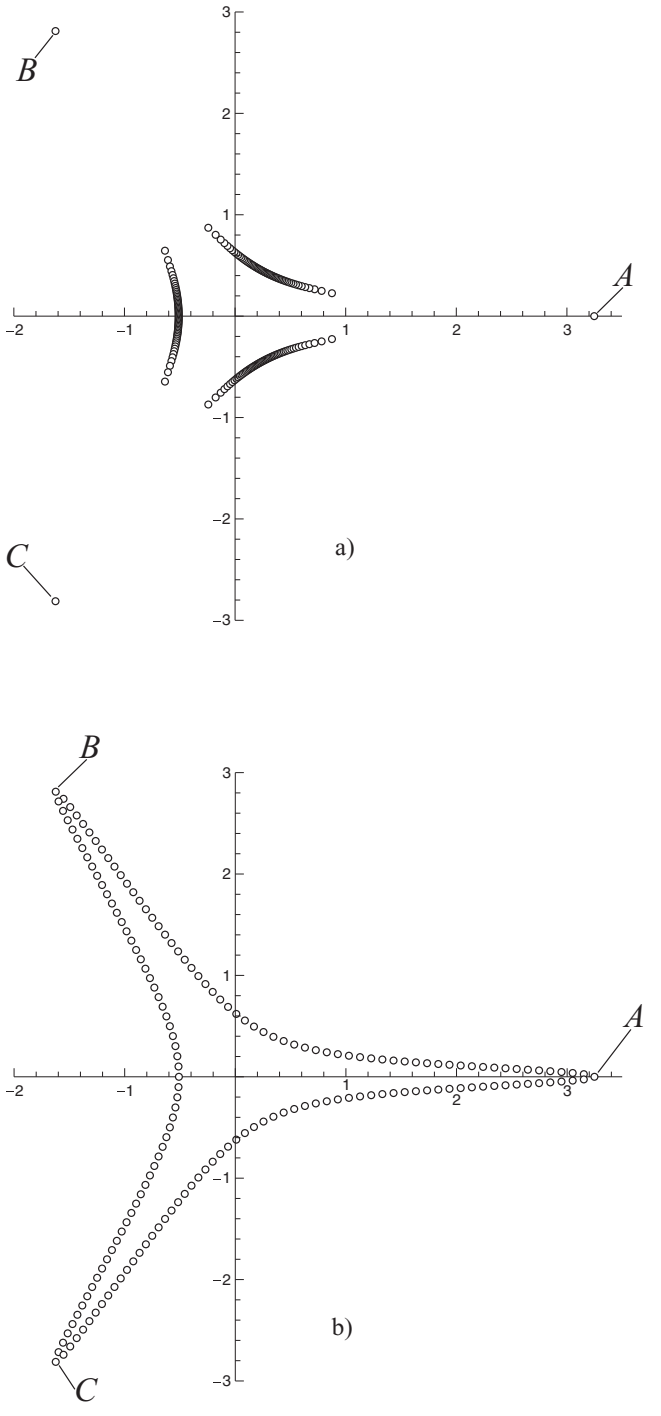

FIGURE 9. Shape of the free surface at t = 1.5: (a) The direct Padé summation; (b) Padé summation after replacement of variables.

https://doi.org/10.1017/S0956792514000242 Published online by Cambridge University Press

of markers on the free boundary. As α changes from 0 to 2π, one turn around the fluid along the free boundary is performed.

To take the integrals

$$S = \int_0^{\theta} |Z_\zeta| d\theta, \qquad S_0 = \int_0^{2\pi} |Z_\zeta| d\theta, \tag{5.3}$$

we have to find the absolute value of the conformal mapping derivative. Differentiating (2.4) with respect to ζ, we obtain

$$Z_\zeta = 1 + 4t\zeta^3 + t^2(-2 + 21\zeta^6) + t^3(-48\zeta^3 + 120\zeta^9) + \cdots. \tag{5.4}$$

Taking into account that $\overline{\zeta} = 1/\zeta$ on the free boundary $|\zeta| = 1$, we find

$$\overline{Z_\zeta} = 1 + 4t/\zeta^3 + t^2\left(-2 + \frac{21}{\zeta^6}\right) + t^3\left(-\frac{48}{\zeta^3} + \frac{120}{\zeta^9}\right) + \cdots. \tag{5.5}$$

We multiply two resultant series (5.4) and (5.5) and then take the square root of the product. As a result, we obtain a series for the absolute value of the conformal mapping derivative:

$$|Z_\zeta| = 1 + \left(\frac{2}{\zeta^3} + 2\zeta^3\right)t + t^2\left(\frac{17}{2\zeta^6} + 2 + \frac{17\zeta^6}{2}\right) + t^3\left(\frac{43}{\zeta^9} - \frac{7}{\zeta^3} - 7\zeta^3 + 43\zeta^9\right) + \cdots.$$

Substituting $\zeta = e^{i\theta}$, we find

$$|Z_\zeta| = 1 + 4t\cos 3\theta + t^2(2 + 17\cos 6\theta) + t^3(-14\cos 3\theta + 86\cos 9\theta) + \ldots \tag{5.6}$$

Using (5.6) for calculating the integrals (5.3), we obtain

$$S = \theta + \frac{4}{3}t\sin 3\theta + t^2\left(2\theta + \frac{17}{6}\sin 6\theta\right) + t^3\left(-\frac{14}{3}\sin 3\theta + \frac{86}{9}\sin 9\theta\right) + \cdots, \tag{5.7}$$

$$S_0 = 2\pi + 4\pi t^2 - \frac{5\pi}{2}t^4 + \cdots. \tag{5.8}$$

Substituting series (5.7), (5.8) into (5.2) and performing their division, we obtain

$$\alpha = \theta + \frac{4}{3}t\sin 3\theta + \frac{17}{6}t^2\sin 6\theta + t^3\left(-\frac{22}{3}\sin 3\theta + \frac{86}{9}\sin 9\theta\right) + \cdots. \tag{5.9}$$

Substituting series (5.9) into the formula $\mu = e^{i\alpha}$, we obtain the change of variables $\mu(\zeta, t)$:

$$\mu(\zeta, t) = \zeta + t\left(-\frac{2}{3\zeta^2} + \frac{2}{3}\zeta^4\right) + t^2\left(-\frac{43}{36\zeta^5} - \frac{4\zeta}{9} + \frac{59\zeta^7}{36}\right) + t^3\left(-\frac{629}{162\zeta^8} + \frac{155}{54\zeta^2} - \frac{257\zeta^4}{54} + \frac{935\zeta^{10}}{162}\right) + \ldots \tag{5.10}$$

If we now find the inverse function $\zeta(\mu, t)$ from series (5.10) and substitute it into (2.4), we obtained the sought series (5.1). However, it is easier to search for the function $Z(\mu, t)$

https://doi.org/10.1017/S0956792514000242 Published online by Cambridge University Press

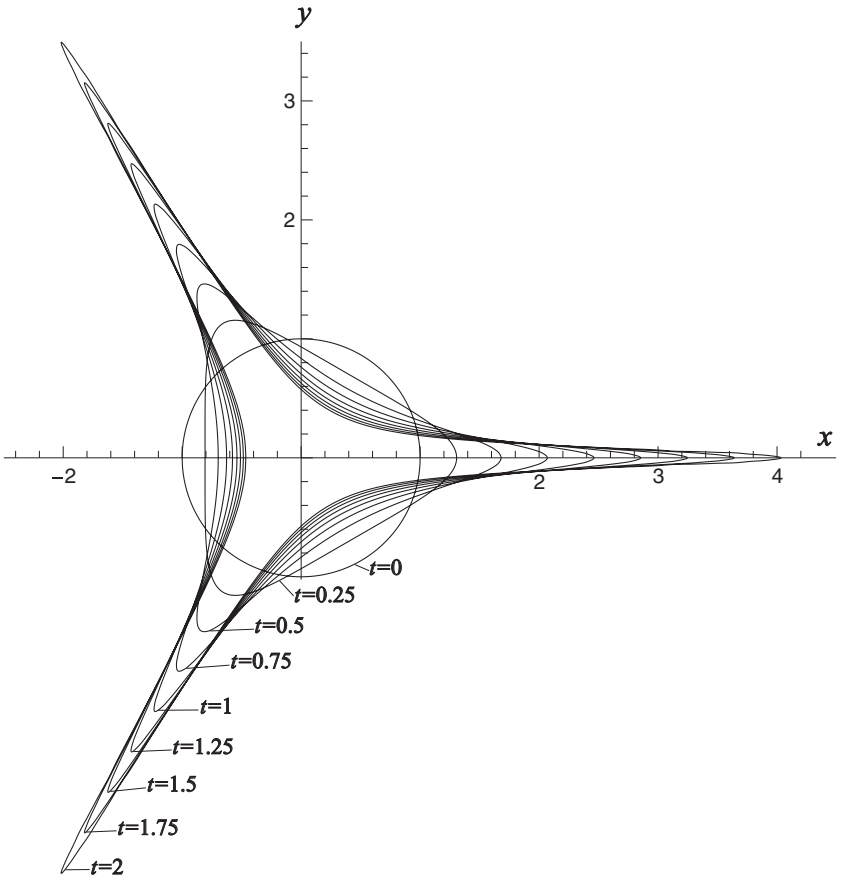

FIGURE 10. Evolution of the free surface with time.

in the following form with undetermined coefficients $a_{i,j}$ directly:

$$Z(\mu,t) = \mu + t(a_{1,-2}\mu^{-2} + a_{1,4}\mu^4) + t^2(a_{2,-5}\mu^{-5} + a_{2,1}\mu + a_{2,7}\mu^7) + t^3(a_{3,-8}\mu^{-8} + a_{3,-2}\mu^{-2} + a_{3,4}\mu^4 + a_{3,10}\mu^{10}) + \cdots. \tag{5.11}$$

The undetermined coefficients can be easily found if we require that the initial series (2.4) is obtained after substituting (5.10) into (5.11).

The shape of the free surface for different times obtained by the Padé summation of series (5.1) is shown in Figure 10. The unit circle transforms to a triangular domain consisting of three jets. Each jet becomes thinner with time. The jet apex (the free boundary point located at the greatest distance from the origin of the coordinate system) initially has a unit velocity. After that, its velocity rapidly increases; in the limit $t \to \infty$, the jet apex moves with the maximum possible velocity equal to 1.57344.

https://doi.org/10.1017/S0956792514000242 Published online by Cambridge University Press

6 Conclusion

A precision semi-analytical method, which allows studying unsteady flows with significant deformations of the free boundary, is proposed. The method is based on the presentation of conformal mapping in the form of a power series in time, which is summed up with the use of the Padé approximants. A certain change of variables is first performed to ensure uniformity of conformal mapping on the free boundary.

In this paper, we consider the simplest problem with a quadratic initial velocity field. However, more complicated formulations can also be considered. An analysis of recurrent boundary-value problems (2.6), (2.7) shows that the following statement is valid here. If $Z_\zeta^{(0)}, U^{(0)}$ are rational functions of ζ, then the functions $Z^{(k)}$ and $U^{(k)}$ ($k \geqslant 1$) are also rational functions. This statement allows unified considerations of a fairly large number of problems. For arbitrary rational initial data, it is always possible to construct an algorithm for consecutive finding of coefficients of power series. If the initial data are not rational functions, it is possible to consider a certain rational approximation and solve a problem close to the posed problem.

Acknowledgements

The authors are grateful to S.P. Suetin for useful discussions.

This work was supported by the Presidium of the Russian Academy of Sciences within the Basic Research Project No. 4.8.

References

[1] Aptekarev, A. I., Buslaev, V. I., Martinez–Finkelshtein, A. & Suetin, S. P. (2011) Padé approximants, continued fractions, and orthogonal polynomials. *Russian Math. Surveys* **66**(6), 1049–1131.

[2] Baumel, R. T., Burley, S. K., Freeman, D. F., Gammel, J. L. & Nuttal J. (1982) The rise of a cylindrical bubble in an inviscid liquid. *Can. J. Phys.* **60**(7), 999–1007.

[3] Belykh, V. N. (1972) The existense and uniqueness theorem the solution of spherical bubble problem. *Dinamica Sploshnoi Sredy*. Lavrentyev Institute of Hidrodynamics, Novosibirsk **12**, 63–76 (in Russian).

[4] Cummings, S. D., Howison, S. D. & King, J. R. (1999) Two-dimensional Stokes and Hele-Shaw flows with free surfases. *Eur. J. Appl. Math.* **10**, 635–680.

[5] Dallaston, M. C. & Mc Cue, S. W. (2010) Accurate series solutions for gravity-driven Stokes waves. *Phys. Fluids* **22**, 082104.

[6] Dirichlet, G. L. (1861) Untersuchungen über ein problem der hydrodynamik. *J. Reine Angem. Math.* **58**, 181–216.

[7] Dyachenko, A. I. (2001) On the dynamic of an ideal fluid with a free surface. *Dokl. Math.* **63(1)**, 115–118; Translated from: *Dokl.Akad. Nauk* **376(1)**, 27–29 (in Russian).

[8] Galin, L. A. (1945) Unsteady filtration with a free surface. *Dokl. Akad. Nauk SSSR* **47**, 246–249 (in Russian).

[9] Gammel, J. L. (1976) The rise of a bubble in a fluid. *Lecture Notes Phys.* **47**, 141–163.

[10] Karabut, E. A. (1986) The use of power series in time in the problem of the motion of cylinder cavity in liquid. I. The finding of coefficients of power series. *Dinamica Sploshnoi Sredy. Lavrentyev Institute of Hydrodinamics, Novosibirsk*. **78**, 56–73 (in Russian).

https://doi.org/10.1017/S0956792514000242 Published online by Cambridge University Press

[11] Karabut, E. A. (1991) Semi-analytical investigation of unsteady free-boundary flows. *Intern. Ser. Numer. Math.* **99**, 215–224.
[12] Karabut, E. A. (1996) Asymptotic expansions in the problem of a solitary wave. *J. Fluid Mech.* **319**, 109–123.
[13] Karabut, E. A. (1998) An approximation for the highest gravity waves on water of finite depth. *J. Fluid Mech.* **372**, 45–70.
[14] Karabut, E. A. (2013) Exact solutions of the problem of free-boundary unsteady flows. *C. R. Mecanique* **341**, 533–537.
[15] Lavrentyeva, O. M. (1980) On the liquid ellipsoid motion. *DAN USSR*. **253**(4), 828–831.
[16] Lavrentyeva, O. M. (1984) About one class of liquid ellipsoid motion. *J. Appl. Mech. Tech. Phys.* **25**(4), 148–153.
[17] Longuet-Higgins, M. S. (1972) A class of exact, time-dependent, free surface flows. *J. Fluid Mech.* **55**(3), 529–543.
[18] Longuet-Higgins,M. S. (1975) Integral properties of periodic gravity waves of finite amplitude. *Proc. R. Soc. London. Ser. A* **342**, 157–174.
[19] Maklakov, D. V. (2002) Almost-highest gravity waves on water of finite depth. *Eur. J. Appl. Math.* **13**, 67–93.
[20] Nalimov, V. I. & Pukhnachov, V. V (1975) *Unsteady Flow of Ideal Liquid with Free Boundary*. Novosibirsk (in Russian).
[21] Nuttal, J. (1980) Sets of minimum capacity, Padé approximants and the bubble problem. In: C. Bardos & D. Bessis (editors), *Bifurcation Phenomena in Mathematical Physics and Related Topics*, Dordrecht, Netherlands, pp. 185–201.
[22] Ovsyannikov, L. V. (1967) General equation and examples. In: *The Problem of the Unstable Flow with a Free Boundary*, Novosibirsk, pp. 5–75 (in Russian).
[23] Ovsyannikov, L. V. (1970) On the bubble emersion. In: *A Some Problems of the Mechanics and Mathematics*, Nauka, pp. 209–219. (in Russian).
[24] Ovsyannikov, L. V. (1971) A planar problem of unsteady free boundary fluid motion. *Dinamica Sploshnoi Sredy*. Lavrentyev Institute of Hidrodynamics, Novosibirsk **8**, 22–30. (in Russian).
[25] Petrov, A. G. (2009) *Analitical Hydrodynamics*, Fizmatlit, Moscow (in Russian).
[26] Polubarinova-Kochina, P. Ya. (1945) On the motion of the oil contour.*Dokl. Akad. Nauk SSSR* **47**, 254–257 (in Russian).
[27] Pukhnachov, V. V. (1978) On the motion of liquid ellipse. *Dinamica Sploshnoi Sredy*. Lavrentyev Institute of Hidrodynamics, Novosibirsk **33**, 68–75 (in Russian).
[28] Stahl, H. (1997) The convergence of Padé approximants to functions with branch points. *J. Approx. Theory*. **91**(2), 139–204.
[29] Titchmarsh, E. C. (1939) *The Theory of Functions*, Oxford University Press.
[30] Van Dyke, M. (1975) Computer extension of perturbation series in fluid mechanics. *SIAM J. Appl. Math.* **28**(3), 720–734.
[31] Van Dyke, M. (1978) Semi-analytical applications of the computer. *Fluid Dynamics Transactions. Warszawa.* **9**, 305–320.
[32] Van Dyke, M. (1981) Successes and surprisec with computer-extended series. *Lecture Notes in Physics.* **141**, 405–410.
[33] Zakharov V. E., Dyachenko A. I. & Vasilyev O. A. (2002) New method for numerical simulation of a nonstationary potential flow of incompressible fluid with a free surface. *Eur. J. Mech.* **21**, 283–291.